

Follistatin Gene Therapy for Sporadic Inclusion Body Myositis Improves Functional Outcomes

Jerry R. Mendell,^{1,2,3} Zarife Sahenk,^{1,2,3} Samiah Al-Zaidy,^{1,2} Louise R. Rodino-Klapac,^{1,2} Linda P. Lowes,^{1,3,4} Lindsay N. Alfano,^{1,3,4} Katherine Berry,^{1,3,4} Natalie Miller,^{1,3,4} Mehmet Yalvac,¹ Igor Dvorchik,⁵ Melissa Moore-Clingenpeel,⁵ Kevin M. Flanigan,^{1,2,3} Kathleen Church,¹ Kim Shontz,¹ Choumpree Curry,¹ Sarah Lewis,¹ Markus McColly,¹ Mark J. Hogan,⁶ and Brian K. Kaspar^{1,2}

¹Center for Gene Therapy, Nationwide Children's Hospital, Columbus, OH 43205, USA; ²Department of Pediatrics, The Ohio State University, Columbus, OH 43205, USA; ³Department of Neurology, The Ohio State University, Columbus, OH 43210, USA; ⁴Clinical Therapies, Nationwide Children's Hospital, Columbus, OH 43205, USA; ⁵Biostatistics Research Core, Nationwide Children's Hospital, Columbus, OH 43205, USA; ⁶Vascular and Interventional Radiology, Department of Radiology, Nationwide Children's Hospital, Columbus, OH 43205, USA

Sporadic inclusion body myositis, a variant of inflammatory myopathy, has features distinct from polymyositis/dermatomyositis. The disease affects men more than women, most commonly after age 50. Clinical features include weakness of the quadriceps, finger flexors, ankle dorsiflexors, and dysphagia. The distribution of weakness is similar to Becker muscular dystrophy, where we previously reported improvement following intramuscular injection of an isoform of follistatin (FS344) by AAV1. For this clinical trial, rAAV1.CMV.huFS344, 6×10^{11} vg/kg, was delivered to the quadriceps muscles of both legs of six sporadic inclusion body myositis subjects. The primary outcome for this trial was distance traveled for the 6-min walk test. The protocol included an exercise regimen for each participant. Performance, annualized to a median 1-year change, improved +56.0 m/year for treated subjects compared to a decline of -25.8 m/year ($p = 0.01$) in untreated subjects ($n = 8$), matched for age, gender, and baseline measures. Four of the six treated subjects showed increases ranging from 58–153 m, whereas two were minimally improved (5–23 m). Treatment effects included decreased fibrosis and improved regeneration. These findings show promise for follistatin gene therapy for mild to moderately affected, ambulatory sporadic inclusion body myositis patients. More advanced disease with discernible muscle loss poses challenges.

INTRODUCTION

The term “inclusion body myositis” (IBM) was originally proposed in 1971 to describe a chronic inflammatory myopathy with intranuclear and intracytoplasmic tubular filaments within muscle fibers.¹ Clinical and pathologic studies over more than four decades have supported this condition as a disorder distinct from other idiopathic inflammatory myopathies.² Incidence and prevalence statistics confirm sporadic IBM (sIBM) to be the most commonly acquired muscle disease after age 50.³ Men are more affected than women (ratio of men to women, 3:1).⁴ The disorder is sporadic with insidious onset and distinctive features suggesting a dual role for both immunopathogenic and ongoing degenerative events. The typical clinical findings include

quadriceps muscle weakness and atrophy, finger flexor and ankle dorsiflexor weakness, and dysphagia. These features distinguish sIBM from other inflammatory myopathies, and diagnostic criteria were initially established by Griggs et al.⁵ and later modified by Hilton-Jones et al.⁶

Inflammation is prominent in sIBM, with similarities to polymyositis.⁷ Intact myofibers are surrounded and invaded by inflammatory cells consisting of macrophages and cytotoxic CD8⁺ T cells and the ubiquitous overexpression of MHC-1 on the surface of muscle fibers.^{8,9} Distinguishing histological hallmarks of sIBM consist of rimmed vacuoles filled with granular material, Congo red-positive amyloid deposits,¹⁰ and 15- to 18-nm tubulofilamentous inclusions seen by electron microscopy. Additional features include ragged red fibers associated with mitochondrial gene deletions,^{11–13} increased numbers of COX-negative fibers, and overexpression of α B-crystallin¹⁴ that associates with amyloid precursor protein (APP)¹⁵ and pro-inflammatory markers indicative of a cell stress response (phosphorylated tau, presenilin-1, apolipoprotein E, γ tubulin, clusterin, α -synuclein, and gelsolin).¹⁶

sIBM has no treatment; weakness is progressive and impairs activities of daily living, with wheelchair dependency by 10 years in most cases.¹⁷ The disease is notoriously refractory to immune suppression.¹⁸ The list of therapeutic failures begins with corticosteroids representing the most frequently used pharmacologic agent to treat sIBM. The logic is apparent given the inflammatory findings on muscle biopsy, but, after decades of research, there is unequivocal agreement supporting the lack of glucocorticoid efficacy in sIBM.^{18–21} Additional therapies have also focused on the possible benefits of immune suppression and include intravenous immunoglobulin in

Received 4 December 2016; accepted 15 February 2017;
<http://dx.doi.org/10.1016/j.ymthe.2017.02.015>.

Correspondence: Jerry R. Mendell, MD, Gene Therapy Center, Nationwide Children's Hospital, 700 Children's Drive, Columbus, OH 43205, USA.

E-mail: jerry.mendell@nationwidechildrens.org

Table 1. Follistatin sIBM Patient Demographics with 6MWT Data before and after Treatment

Subject	Age at Onset (years)	Age at GT (years)	Baseline 6MWT (m)	Final 6MWT (m)	6MWT Change from Baseline (m)	Duration of Follow-Up (months)
1	50	59.6	459	464	5	24.0
2	61	66.7	385	494	108	24.0
3	70	72.4	402	424	23	2.0
4	65	72.7	500	567	67	16.0
5	62	63.0	428	486	58	12.0
6	63	65.1	498	651	153	12.0
Median	62.5	65.9	443.5	490	62.5	14.0

GT, gene therapy. The median for age, baseline, and final distance on 6MWT and change from baseline are shown for each subject.

randomized clinical trials,^{22,23} β -interferon-1a,^{24,25} methotrexate,²⁶ anti-thymocyte globulin,²⁷ etanercept,²⁸ alemtuzumab,²⁹ and simvastatin.³⁰ In addition, initial attempts to inhibit myostatin using an antibody, bimagrabumab, to block the Activin IIB receptor looked favorable³¹ but later failed in a phase II/III clinical trial (Novartis, April 21, 2016).

In 2008, we laid the foundation for an alternative strategy to treat sIBM based on the knowledge that disruption of myostatin, also known as the growth and differentiation factor 8 (GDF-8) gene in wild-type mice, resulted in a widespread increase in skeletal muscle mass.³² The muscle-building effects of follistatin (FS) were even more profound, as demonstrated in myostatin (*Mstn*^{-/-}) knockout mice that carried the FS transgene, making it an attractive target for translation.³³ In clinical application, the alternatively spliced FS cDNA isoform FS344, preferred because of minimal effects on the hypothalamic-pituitary-gonadal axis,^{34,35} proved to be safe and effective in an intramuscular gene transfer trial to the quadriceps muscle in Becker muscular dystrophy.³⁶ Based on these findings, a similar gene transfer study of rAAV1.CMV.huFS344 to the quadriceps muscle was initiated for sIBM. Although weakness between Becker muscular dystrophy and sIBM has a similar distribution in the lower limbs, the results in a traditionally refractory inflammatory, vacuolated myopathy were less predictable.

RESULTS

Study Design

The baseline characteristics of the six male participants are outlined in Table 1. Each fulfilled previously published diagnostic criteria⁵ and conditions defined in Investigational New Drug (IND) 14845. The Institutional Review Board at Nationwide Children's Hospital approved the clinical trial protocol that was registered at ClinicalTrials.gov. The protocol followed the Helsinki Declaration, and all patients gave their written informed consent prior to participation. The study was designed to target sIBM ambulatory patients with knee extensor weakness (Medical Research Council [MRC] grade 4).³⁷ All were 50 years of age or older (62.5 median age) at the time of disease onset, with gene transfer at a median age of 65.9 years. Serum neutralizing antibody titers to adeno-associated virus (AAV)1, assessed by ELISA, had to be below 1:50 at the start of the

study and were monitored according to a previously published clinical trial schedule.^{38,39}

T cell responses toward AAV1 capsid and follistatin were monitored by interferon γ (IFN- γ) enzyme-linked immunospot (ELISpot) assay and were below 50 spot-forming cells/million peripheral blood mononuclear cells (PBMCs) prior to enrollment.^{38,39} Study participants underwent an initial screening visit to establish criteria for enrollment, and this included a pre-treatment muscle biopsy. Prednisone (60 mg daily) was started 2 weeks later and continued for 1 month prior to rAAV1.CMV.huFS344 injections as a precaution against an immune response to the AAV capsid, especially in light of the underlying inflammatory milieu in sIBM. The prednisone dose was maintained for approximately 30 days after gene delivery. Muscle biopsies provided a histopathological assessment of muscle at baseline to compare with a follow-up biopsy on the opposite extremity on day 180 after gene transfer. The extremity undergoing initial biopsy was chosen by a randomization table and taken from the proximal vastus lateralis, thus determining the post-biopsy site in the opposite extremity targeting the same head of the quadriceps. Serum chemistry/hematology batteries were assessed at baseline, on days 7, 14, 30, 60, 90, and 180, and yearly to evaluate adverse effects because of gene transfer and included complete blood count, liver function studies, kidney function (cystatin C),⁴⁰ amylase, creatine kinase, and serum hormones (follicle-stimulating hormone [FSH], leutinizing hormone [LH], testosterone, and estrogen).

rAAV1.CMV.huFS344 was prepared and delivered by the research pharmacist at Nationwide Children's Hospital (NCH) to the procedure room at the time of gene transfer on ice (not frozen) and administered to the subject within 8 hr of preparation. Handling of the rAAV1.CMV.huFS344 gene followed compliance standards for biosafety level 1 vectors.³⁹ The final volume to the quadriceps muscle of each limb was diluted in 6 mL of lactated Ringer's (1 mL per syringe). The exact sites of gene injections in the heads of the quadriceps muscle were chosen by pre-treatment magnetic resonance images scored according to the modified Hawley scoring system, which has shown good correlation with histological findings in previous studies.⁴¹⁻⁴³ The sites of the vastus medialis (VM), rectus femoris (RF), and vastus lateralis (VL) marked for injection were those best

Table 2. Comparison of 6MWT following FS344 Gene Therapy

Group	Baseline 6MWT (m)	Final 6MWT (m)	Change from Baseline (m)	Annualized Change ^a (m)
Treated group (n = 6)	443.5 (402.0, 498.0)	489.5 (464.0, 567.0)	+62.5 (23.0, 108.0)	+56.0 (50.3, 138.0)
Untreated group (n = 8)	459.0 (439.5, 469.0)	420.0 (388.5, 447.5)	-33.0 (-77.0, -8.0)	-25.8 (-57.6, -7.9)
p Values	0.59	0.01	0.001	0.001

All values are expressed as median (25th percentile, 75th percentile).

^aThe performance of the subjects was annualized to a median change over 1 year.

preserved with the least fibrosis and fat replacement. At the time of injection, 12 sites of the best preserved regions of quadriceps each received 0.5 mL of vector that was further guided by a Myoject Luer lock electromyography (EMG) needle electrode that recorded compound muscle action potentials to ensure that viable muscle was present at the site of delivery.

A novel protocol design was introduced, taking advantage of observations from the follistatin Becker muscular dystrophy gene therapy trial showing that the most active patients in that trial achieved the best results on the 6-min walk test (6MWT).³⁶ Additional studies by Hansen et al. demonstrated that exercise induces a marked increase in plasma follistatin.⁴⁴ For this sIBM gene therapy trial, each patient was encouraged to exercise up to his or her own tolerance three times per week, but, at a minimum, he or she should ride a stationary bicycle for 15 min and perform knee extension leg lifts with a 5-pound ankle weight (three repeats of ten leg extensions) three times per week.

Functional Response to Treatment

Table 1 shows the baseline and final distance in meters on the 6MWT for each subject (n = 6). The treated patients were followed at regular intervals for 1–2 years. Patient 3 could no longer participate in testing 2 months after gene therapy because of a fall that resulted in a concussion and a torn hamstring muscle. Because this was an intent-treat analysis, his data were included up to the point of injury. To standardize reporting of the results, the performance of subjects (Table 1) was annualized to a median 1-year change to provide a standard score for comparison across the lengths of follow-up between subjects (Table 2). Treated subjects (n = 6) improved +56.0 m/year (+4.7 m/month), whereas a cohort of untreated sIBM patients (n = 8) followed in our Neuromuscular Clinic matched for age, gender, and baseline 6MWT decreased by -25.8 m/year (-2.1 m/month) (p = 0.01) (Table 2; Figure 1). Secondary motor outcomes, including “Timed Up and Go” and “Ascending 4 Stairs” are shown at 1 year after gene therapy for all subjects (Table S1). This time point is comparable for all participants except for subject 3, who fell 2 months after gene transfer. Ascending stairs improved for all patients, and four patients improved in “Timed Up and Go”.

A variable in this study that appeared to influence the outcome was exercise. At each visit, participants turned in a log of their exercise regimen. The patients reporting the most intense exercise routines (exceeding the recommended minimum) improved by 108 m (sub-

ject 2) and 153 m (subject 6) compared to baseline (Table 1). These two patients, plus subjects 4 and 5, reported greater exercise tolerance and improved activities of living following gene delivery. Peak follistatin levels did show a correlation with improvement in the 6MWT (Figure S1).

No adverse events (AEs) or serious AEs (SAEs) were encountered related to gene therapy (Table S2). As in our prior report for Becker muscular dystrophy follistatin gene therapy, we found no changes in pituitary-gonadal hormone levels (FSH, LH, estrogen, or testosterone) or any organ system assessment of the heart, liver, kidney, or bone marrow by physical exams or repeated chemistries throughout the study. Assessment of the IFN- γ ELISpot assay for T cell immune responses to the AAV1 capsid showed no consistent pattern of T cell immunity, and serum follistatin antibody levels remained below 1:50 titers. Patients with sIBM are subject to falling because of weakness of the quadriceps muscles that results in knees giving way. As reported above, subject 3 had a fall that resulted in an SAE of a concussion and torn hamstring, which prevented him from finishing the motor assessment (he was followed for other adverse events). Subject 4 had two SAEs that prevented testing at two time points. The first was due to a biking accident, and the second was due to a fall that required several weeks of rehabilitation. He recovered from both and was able to participate in motor assessments, increasing his 6MWT by 67 m 16 months after gene transfer (Table 1).

Muscle Biopsy Findings

We compared muscle biopsies 30 days prior to and 6 months after gene transfer. Two patients (5 and 6) had microscopic slides of paraffin-embedded muscle from a previous biopsy, and we chose not to obtain another pre-treatment biopsy (muscle biopsy findings were an exploratory outcome for this trial). Quantitative pre- and post-treatment measures were restricted to tissue processed in our laboratory (subjects 1–4). All post-treatment biopsies demonstrated an increase in the number of muscle fibers per square millimeter area and a decrease in the endomysial connective tissue and fat content and the inflammatory component. The histologic appearance of muscle following follistatin treatment (Figure 2) shows normalization of fiber size appearance and distribution, decreased central nuclei, and significantly diminished muscle fibrosis in three of the four post-treatment biopsies (Figures 3A–3C). Moreover, we found downregulation of the expression levels of the fibrosis markers transforming growth factor β (TGF- β), collagen 1A (Col1A), and fibronectin in

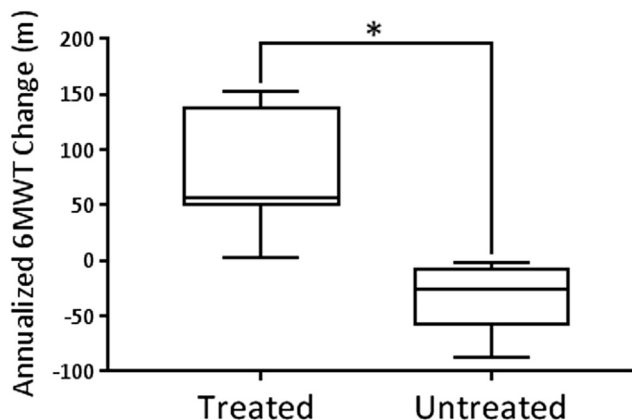


Figure 1. Annualized 6MWT Change in Treated versus Untreated sIBM Groups

Shown is a comparison of the median annualized change in the distance walked in the 6MWT over 1 year following rAAV1.CMV.huFS344 treatment of sIBM (treated group, $n = 6$) versus the untreated sIBM control group matched for age, gender, and baseline 6MWT. Treated subjects improved $+56.0$ m/year, whereas untreated patients' performance decreased by -25.8 m/year ($p = 0.01$). Results per subject are shown in Table 1 and Figure S1.

the post-treatment biopsies correlating with these histopathological improvements (Figure 3D).

These findings collectively suggested that the treatment established a more uniform and normalized size distribution; i.e., improved radial growth of fibers resulting from enhanced muscle regeneration. Because mammalian target of rapamycin complex 1 (mTORC1) is the major activator of radial growth/protein synthesis in muscle,⁴⁵ we then investigated whether mTORC1 was activated by the follistatin gene therapy as previously reported.⁴⁶ The activity of mTORC1 was assessed by the phosphorylation levels of its substrates, eukaryotic translation initiation factor 4E-binding protein 1 (4E-BP1) and the ribosomal protein S6 kinase1-targeted protein (S6P), using western blot analysis. The phosphorylated S6P and 4E-BP1 levels were higher in the post-treatment samples, compatible with ongoing, increased protein synthesis 6 months after treatment compared with baseline pretreatment samples (Figure 4). We also found a decrease in the phosphorylated levels of the cell stress sensor AMP-activated protein kinase (AMPK) in response to follistatin treatment.^{47,48}

DNA copy number at the site of the biopsy is shown in Table S3 for each patient undergoing treatment.

DISCUSSION

Myostatin is a muscle-specific secretory protein that regulates muscle growth.¹ We have chosen to use follistatin to inhibit the myostatin signaling pathway for sIBM for several reasons. First, we were previously able to demonstrate both safety and a therapeutic benefit following gene delivery using AAV1.CMV.huFS344 in Becker muscular dystrophy.³⁶ We found a functional increase in the 6-min

walk distance (6MWD) without adverse events. These findings established a potential path for treatment of sIBM, a significantly different condition, even though the distribution of muscle weakness has similarities. sIBM is an enigmatic condition with ongoing debates about pathogenesis: is it predominantly inflammatory versus primarily a myopathic or a degenerative disease with secondary inflammation? Follistatin as a therapeutic tool for treatment of sIBM has three potential mechanisms to combat crucial aspects on both sides of the debate. First, follistatin binds to activins inhibiting the release of pro-inflammatory cytokines and precluding the development of monocyte/macrophages, myeloid dendritic cells, and T cell subsets, all potentially contributing to sIBM.⁴⁹ Further benefits result from a reduction in muscle fibroblast proliferation stimulated by myostatin inhibition.^{50,51} As predicted, in our study, the post-treatment biopsies showed histological evidence of decreased fibrosis along with down-regulation of the expression levels of the fibrosis markers TGF- β , Col1A, and fibronectin, providing direct evidence for this effect of follistatin. In sIBM, it is highly unlikely that we could achieve a therapeutic benefit without reducing fibrosis. The third arm that provides a favorable environment for upregulating follistatin in chronic muscle disease is its ability to stimulate myoblasts to express MyoD, Myf5, and myogenin, all myogenic transcription factors that promote muscle regeneration.⁴⁵ Moreover, follistatin-mediated increased muscle mass and force-producing capacity is concomitant with mTOR activation and increased protein synthesis independently of myostatin-driven mechanisms. It has been shown that Smad3/Akt/mTOR/S6Kinase1/2/S6P signaling plays a critical role in this process.⁴⁶ Our findings of an overall increased activity in mTORC1 in the post-treatment biopsies, assessed by increased phosphorylation levels of its substrates, 4E-BP1 and S6K1-targeted ribosomal protein S6P, provide the first in vivo evidence in patients for these biological effects of follistatin. Ultimately, the combined effect of reducing fibrosis and inflammation while promoting muscle cell regeneration supports a favorable milieu for muscle recovery, as seen in this translational gene therapy clinical trial. It is also important to add that the combination of a glucocorticoid effect received by sIBM subjects for about 60 days, in the presence of exercise and follistatin upregulation, could have influenced outcomes. An interesting possibility is that the upregulation of Akirin1 expression in the presence of suppression of myostatin following FS344 gene delivery provided a contributory path for muscle growth. Glucocorticoids usually suppress the ability of satellite cells to promote muscle growth, accounting for steroid-related muscle atrophy. However, a paradoxical effect is seen from the combinational effect of follistatin and steroid therapy, resulting in myostatin inhibition, increased Akirin1 expression, and potentiation of muscle regeneration.⁵²

Another interesting arm of the therapeutic efficacy illustrated in this clinical gene therapy trial is the benefit of a combined gene delivery of follistatin with a muscle contraction exercise program. In the follistatin Becker muscular dystrophy gene therapy trial, we thought that patients who reported a continued ability to adhere to active schedules were those who improved most consistently in the 6MWT.³⁶ There is also clear evidence from prior studies in patients and in mice that

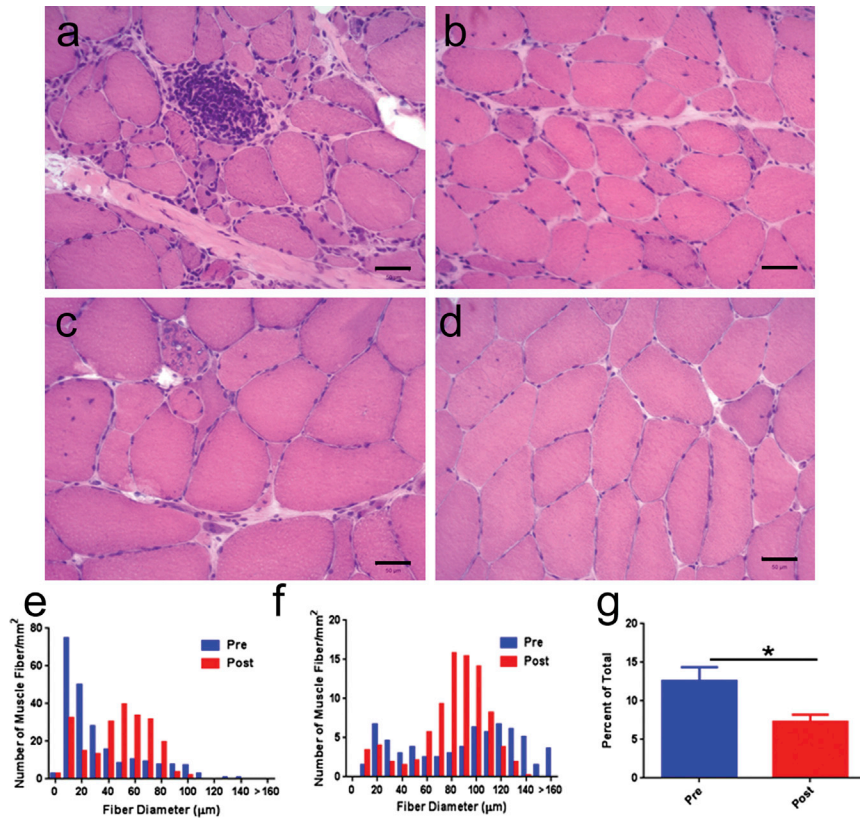


Figure 2. Histopathology in Pre- and Post-follistatin Treatment Muscle Biopsies

(A–D) Representative H&E-stained cross sections from the pre-follistatin (A and C) and post-follistatin (B and D) muscle biopsies for subject 2 (A and B) and subject 4 (C and D). Both subjects improved in their distance walked on the 6MWT (Table 1). Post-treatment samples show fewer small basophilic regenerating fibers, less variation in fiber size, and fewer central nuclei. (E and F) The fiber size histograms for subject 2 (E) and subject 4 (F) illustrate a decrease in small fiber subpopulation and a shift toward normalization of fiber size distribution with an increase in the number of fibers within the normal size range. (G) Quantification of multinucleated fibers as percent of total number of fibers with internal nuclei showed a significant reduction in the post-treatment samples, suggestive of normalization of the internal cytoarchitecture. * $p = 0.0267$ by two-tailed t test.

expression of follistatin increases with exercise.⁴⁴ The exercise regimen we recommended in this clinical trial was modest: riding a stationary bicycle for 15 min and knee extensor leg lifts with a 5-pound weight while in a sitting position (three sets of ten) three times per week on alternating days. We monitored the program with patient-recorded logs that were brought to the clinic at each follow-up appointment. Four subjects followed the exercise program with little variation (subjects 2, 4, 5, and 6) and also voluntarily performed additional exercises (especially subjects 2 and 6; Table 1; Figure S1). These are the subjects who were found to have the greatest gains in the 6MWD. It is also important to note that all patients in this study improved in outcome measures, but the difference was striking between the exercise cohort (subjects 2, 4, 5, and 6) and the non-exercise cohort (subjects 1 and 3) while the dose of rAAV1.CMV.huFS344 remained the same for all participants. A question could be raised regarding efficacy entirely related to exercise, but we believe this to be highly unlikely given the failure of exercise alone (including 10-m and 30-m walk, timed-up-and-go, stair climbing) to improve function in the absence of follistatin therapy.^{53,54} Future follistatin gene therapy clinical trials in muscle diseases of varying causes might benefit from a combined exercise-gene therapy regimen.

The profile of the follistatin isoform FS344 delivered by intramuscular injection to sIBM patients confirmed the safety of the prior Becker muscular dystrophy study using the same cassette. The sIBM patients

had the advantage of a uniform, higher dosing schedule of 6×10^{11} vector genomes (vg)/kg/leg in all subjects. There were no treatment-related AEs or SAEs. Unrelated AEs occurred in two subjects (6%), characterized as falls, and one subject (3%) had a biking accident. It is worth pointing out that this subject continued to show functional improvement despite the injuries that would usually result in further decline

in this disease, suggesting an enhanced muscle-regenerative capacity based on follistatin gene transfer. Other unrelated adverse events are provided in Table S2. No serum chemistry or hormone abnormalities were seen, including gonadotropins, testosterone, or estrogen levels, following gene therapy. There was no consistent pattern of T cell immunity specific to the AAV1 capsid pool, as evaluated by ELISpot assays, and serum anti-follistatin antibody levels remained below 1:50 titers.

In conclusion, this is the first clinical trial to show clear evidence of a treatment benefit in sIBM. This is an important step for this disease, and further studies are warranted. Questions continue regarding how long the treatment benefit will persist and in what range of severity we can expect to see improvement. Obviously, the treatment paradigm must also be extended to include females before we can assess the full effect of follistatin gene delivery for sIBM. In addition, the sIBM patients treated in this trial were ambulatory and relatively mildly affected. More severely affected patients might benefit from systemic delivery. This trial was unequivocally safe and, combined with our prior results in Becker muscular dystrophy, continues to support follistatin gene therapy for muscle disease delivered by AAV.

MATERIALS AND METHODS

Vector Production

The AAV1 vector product was produced as previously described using the human follistatin gene flanked by AAV2 inverted terminal

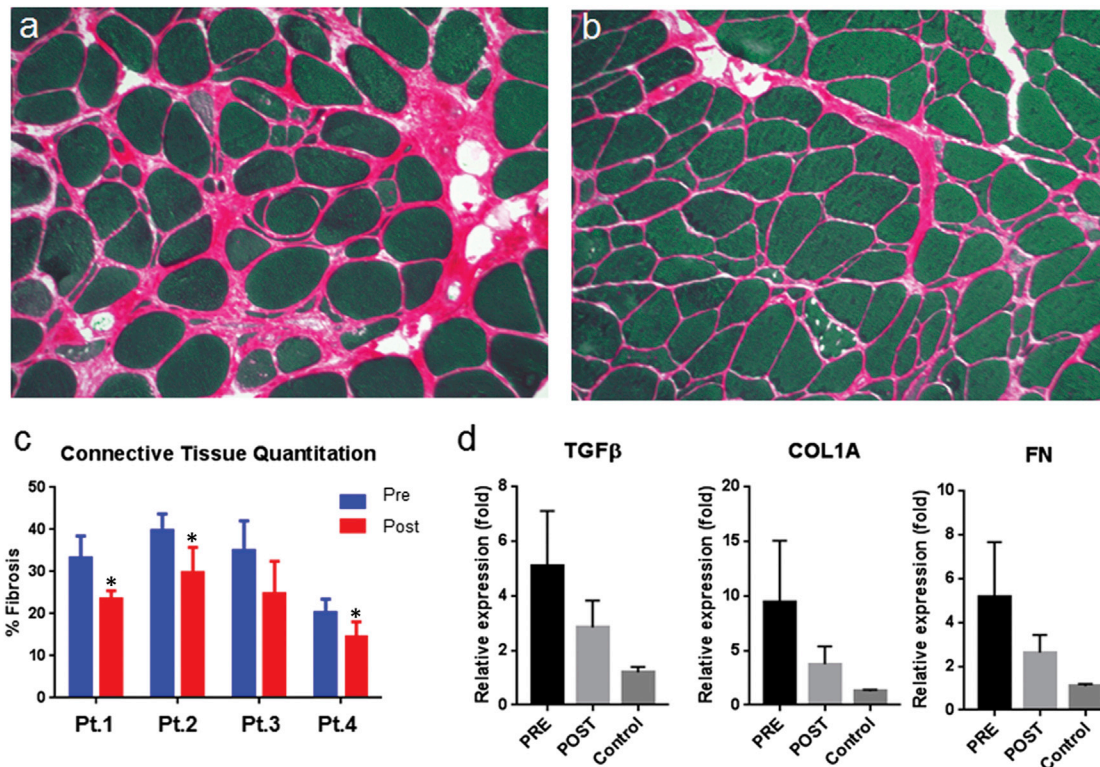


Figure 3. Reduced Fibrosis after Follistatin Gene Therapy

(A–C) Representative cross-sections stained with picrosirius red from pre-treatment (A) and post-treatment (B) biopsies. The quantification of endomysial connective tissue in pre- and post-treatment biopsies is shown as percent fibrosis for individual patients (patients 1–4) (C). Significance (* $p < 0.05$) was assessed by two-tailed *t* test. Error bars represent mean + SEM. (D) Expression levels of fibrosis markers evaluated from quadriceps muscles: TGF- β , Col1A, and fibronectin pre- and post-gene therapy ($n = 4$ in each) versus normal control ($n = 3$). Error bars represent \pm SEM (reduced but not significant because of pretreatment variability).

repeat (ITR) sequences and encapsidated into AAV1 virions.³³ The construct contains the cytomegalovirus (CMV) immediate early promoter/enhancer and uses the β -globin intron for high-level expression. All plasmids used in the production process were produced by Aldevron under its Good Manufacturing Practice Source (GMP-S) quality system and infrastructure. rAAV1.CMV.huFS344 was produced in the Nationwide Children’s Viral Vector GMP manufacturing facility. Release testing, including the final fill product, was performed by our quality assurance unit (QAU). Certificates of stability and analysis were submitted to and approved by the Food and Drug Administration (FDA).

MRI for Guidance of Gene Transfer Sites

The MRI studies completed were non-contrast-enhanced images obtained from both legs, collected at baseline and 6 months after gene therapy treatment for all subjects. Axial T1-weighted images of the lower extremities to the knees were analyzed for injection sites. The MRI studies were scored using the modified Hawley system, which has been validated in previous studies and has shown good correlation with histological findings.^{41–43} Areas of skeletal muscle with a baseline score of 2a or less were targeted. Two of the study investigators evaluated the pre-treatment MRI, a radiologist (M.H.) as well as a

neurologist (S.A.), and they came to a consensus of preserved areas of skeletal muscle that were marked as injection sites.

Muscle Biopsy Analysis

For each patient, pre- and post-treatment quadriceps muscle biopsies, processed according to our well established protocols at NCH, were used for quantitative histopathology, real-time qPCR, and western blot analyses, with the exception of two pre-treatment biopsies performed previously elsewhere (subjects 5 and 6), from which only the microscopic slides were available. H&E-stained cross-sections were used for fiber size measurements and counts of central nuclei. A mean total area analyzed per biopsy was $2.25 \pm 0.43 \text{ mm}^2$, derived from randomly obtained $20\times$ images. Fiber diameters were recorded with a calibrated micrometer using the AxioVision 4.2 software (Zeiss). Fiber size distribution histograms were expressed as number per square millimeter. In random images, the number of fibers with one or more internal nuclei and the percent of fibers with internal nuclei were determined. Quantification of endomysial and perimysial connective tissue was limited to pre- and post-treatment biopsies done at NCH using picrosirius red stains (Abcam, ab150681) (patients 1, 2, 3, and 4). The level of fibrosis was analyzed on $20\times$ photographs using ImagePro software from 12 randomly selected fields in

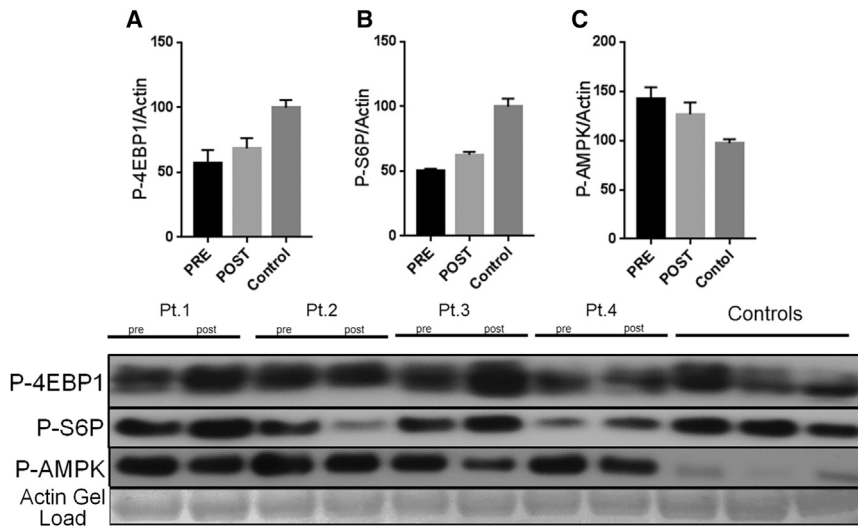


Figure 4. Western Blot Analysis of mTOR and AMPK Signaling before and after Gene Transfer

(A–C) Representative western blot images and analysis of mTOR and AMPK signaling in pre- and post-treatment quadriceps muscles of four subjects and normal control quadriceps muscles. Quantitation of mTOR targets are shown: (A) P-4EBP1^(Thr37/46), (B) P-S6P S6P^(Ser235-Ser236), and (C) P-AMPK^(Thr172). The results in (A) and (B) show increased expression levels of the phosphorylated form of proteins normalized to actin and expressed as percent of normal muscle values. The results in (C) show reduction after treatment. Error bars represent mean + SEM, showing trends following treatment without reaching significance. n = 4 in the pre- and post-treatment groups, and n = 3 in the normal muscle control group.

pre- and post-treatment biopsies. The red area (representing the fibrotic area) was expressed as percent of total area in each image, and the mean ± SEM was determined to represent each biopsy.

qPCR Experiments

The genomic DNA and RNA were extracted from fresh-frozen muscle biopsies using the QIAGEN QIAamp DNA mini kit (#51304) and High Pure RNA isolation kit (Roche, #11828665001), respectively. cDNAs were synthesized using the Transcriptor First Strand cDNA synthesis kit (#04379012001). Standard real-time qPCR was performed to quantify the number of vector genome copies per microgram of genomic DNA using Fast SYBR Green Master Mix (Thermo Fisher Scientific, catalog no. 4385612) according to the manufacturer's instructions. Primers for the CMV promoter were as follows: F 5'-GTTTGACTCACGGGGATTTC-3', R 5'-GGCGGA GTTGTTACGACATT-3'. The pAAV.CMV.FS344 plasmid vector³⁶ was serially diluted for making a standard curve. Other qPCR experiments were performed by using iTaq Universal SYBR Green Supermix (Bio-Rad, #1725122). Primer sequences for TGF-β (F: GGA AATTGAGGGCTTTCGCC, R: CCGGTAGTGAACCCGTTGAT), COL1A (F: CCCCAGAGGCTCTGAAGGTC, R: GGAGCACCAT TGGCACCTTT), and fibronectin (F: ACAAACACTAATGTAA TTGCCCA, R: CGGGAATCTTCTGTGTCAGCC) were designed using NCBI's Primer Blast. All qPCR experiments were done by using the ABI 7500 real-time PCR machine, and the results were computed and analyzed using Data Assist Software (ABI).

Protein Extraction and Western Blot Analysis

For the western blot analysis, fresh-frozen muscles samples were homogenized in radioimmunoprecipitation assay (RIPA) lysis buffer (Thermo Fisher Scientific, #89900) with 1× Halt protease inhibitor (Thermo Fisher Scientific, #78429) and 1× phosphatase inhibitor (Sigma, P0044). The same amount of protein for each sample was loaded on 4%–12% Bolt Bis-Tris Plus precast polyacrylamide gels (Thermo Fisher Scientific, #NW04120BOX) and

transferred to polyvinylidene fluoride (PVDF) membranes (GE Healthcare, #10600021). The following antibodies were used: from Cell Signaling Technologies, anti-phospho S6P^(Ser235-Ser236) (#4858), anti-phospho^{4EBP1(Thr37/46)} (#2855), and anti-phospho AMPK^(Thr172) (#2535); from Santa Cruz Biotechnology, anti-Actin H-300 (#10731). The secondary antibody was anti-rabbit (HAF008) immunoglobulin G (IgG) conjugated with horseradish peroxidase (HRP) (R&D Systems). Specific signals were developed using Amersham ECL Prime western blot detection reagent followed by exposure to X-ray films (Denville, #E3018). Bands on the film were pictured using a camera (Sony A600), and the band intensities were quantified using Quantity-One software (Bio-Rad). The relative content of the analyzed protein band in each sample was determined by normalizing band intensities to the content of Actin in the same sample.

IFN-γ ELISpot Analysis

ELISpot assays were performed on fresh PBMCs as previously described using AAV1 capsid peptide pools and follistatin.³⁶ Concanavalin A (Sigma) served as a positive control and 0.25% DMSO as a negative control. Human IFN-γ ELISpot kits were purchased from U-CyTech. After the addition of PBMCs and peptides, the plates were incubated at 37°C for 48 hr and then developed according to the manufacturer's protocol. IFN-γ spot formation was counted using a Cellular Technologies Limited systems analyzer.

Anti-AAV Neutralizing Antibody Titers

The assay is based on the ability of neutralizing antibody (Nab) in serum to block target cell transduction with a β-galactosidase (β-gal) reporter vector stock. C12 rep-expressing HeLa cells (Viral Vector Core, Nationwide Children's Hospital) were plated in a 96-well plate (Corning) at a concentration of 5e4 cells/well. Plates were incubated at 37°C with 5% CO₂. The following day, an aliquot of patient serum was heat-inactivated for 30 min at 56°C. The serum was diluted in duplicate 2-fold with DMEM in a 96-well plate so that the plate contained 1:50–1:1,638,400 dilutions. 5e7 DNase-resistant

particles (DRPs)/mL AAV1.CMV.β-gal virus was added to the serially diluted wells in a volume of 25 μL. For the assay cutoff, 25 μL of 5e7, 1e7, and 5e6 DRPs/mL were added to other wells containing 1:50 diluted naive serum. The 96-well plates were then rocked for 2–5 min and incubated for 1 hr at 37°C. The medium was then removed, and all 50 μL of the diluted serum/AAV1 complexes was added to the corresponding well containing C12 cells. 50 μL of the Ad5 (MOI = 250) was added to the diluted serum samples. After overnight incubation at 37°C, the medium was replaced with 10% fetal bovine serum (FBS) and DMEM. The medium was removed after 36 hr and gently washed with 200 μL/well of PBS (Invitrogen). 100 μL/well of Pierce β-gal assay reagent (Thermo Fisher Scientific) was added and incubated for 30 min at 37°C. The plates were then read at 405 nm on a SPECTRAMax M2 plate reader (Molecular Devices). The 5e6 DRPs/mL positive control was the assay cutoff, which represents an equivalent of 10% infection and 90% neutralization. The furthest serum dilution producing an average absorbance at 405 nm, which was less than the average absorbance of the 5e6 DRPs/mL positive control, was considered the anti-AAV1 titer.

Anti-follistatin Antibody Titers

An ELISA was performed to measure the level of circulating anti-follistatin antibody in plasma. Briefly, Immulon-4 96-well plates (ISC BioExpress) were coated with 100 μL of human follistatin protein in carbonate buffer (pH 9.4; Pierce) per well. Plates were sealed overnight at 4°C. Plates were blocked with 280 μL per well of 5% nonfat dry milk and 1% normal goat serum (Invitrogen) in PBS for 3 hr at 25°C. Patient plasma was diluted at a 1:50 ratio in solution identical to the blocking solution, and 100 μL was added in duplicate to both wells coated with follistatin in carbonate buffer and wells coated with carbonate buffer alone. Plates were incubated at 25°C for 1 hr.

Statistical Analyses

GraphPad Prism software was used for all statistical analyses. For all comparisons, two-tailed Student's *t* test was used, or, where appropriate, one-way ANOVA was applied.

A value of *p* < 0.05 was considered statistically significant. Distances walked were annualized to a median change per year to provide a standard score for comparison across different lengths of follow-up (**p* = 0.01).

SUPPLEMENTAL INFORMATION

Supplemental Information includes one figure and three tables and can be found with this article online at <http://dx.doi.org/10.1016/j.ymthe.2017.02.015>.

AUTHOR CONTRIBUTIONS

J.R.M., Z.S., and B.K.K. designed the trial. J.R.M. was the principal investigator for the trial, and Z.S., S.A., L.R.K., M.J.H., L.P.L., L.N.A., K.B., and N.M. were sub-investigators for the trial. B.K.K. was critical for product development. J.R.M., S.A., and Z.S. conducted all physical exams. Z.S. performed muscle biopsies for all patients with the assistance of J.R.M. S.A. analyzed all MRI images. Z.S. per-

formed all molecular and pathology review analyses. L.R.K. performed all molecular and immunology review analyses. S.L. processed, sectioned, and stained all muscle biopsies and performed all tissue allocations. K.S. performed all morphometric analyses of the muscle biopsy tissue, measured all fiber diameters, and counted internal nuclei. K.S. performed all ELISAs to measure follistatin levels. M.Y. analyzed all muscle biopsies for mTORC through multiple assays. L.P.L., L.N.A., K.B., and N.M. measured all physical therapy outcomes. M.J.H. guided gene delivery with ultrasound and MRI. K.M.F. assisted gene delivery guidance with the use of EMG. M.M. performed coordinator responsibilities. K.C. and C.C. were liaisons with regulatory oversight. I.D. and M.M.C. performed all statistics. The manuscript was reviewed, edited, and approved by all authors.

CONFLICTS OF INTEREST

B.K.K. had intellectual property filed through Nationwide Children's Hospital and an equity interest related to work that is licensed to Milo Biotechnology. B.K.K. also serves as a paid consultant for Milo. The relationships are managed through a conflict management plan.

ACKNOWLEDGMENTS

The Parent Project Muscular Dystrophy supported the clinical trial. Staff for this trial and some of the materials and supplies were provided by the Senator Paul D. Wellstone Muscular Dystrophy Research Center, NICHD, NIH (5U54HD066409-05). Jesse's Journey supported some of the participating staff. The Myositis Association helped bring this trial to the clinic by supporting the preclinical studies.

REFERENCES

1. Yunis, E.J., and Samaha, F.J. (1971). Inclusion body myositis. *Lab. Invest.* 25, 240–248.
2. Dalakas, M.C. (2010). Inflammatory muscle diseases: a critical review on pathogenesis and therapies. *Curr. Opin. Pharmacol.* 10, 346–352.
3. Wilson, F.C., Ytterberg, S.R., St Sauver, J.L., and Reed, A.M. (2008). Epidemiology of sporadic inclusion body myositis and polymyositis in Olmsted County, Minnesota. *J. Rheumatol.* 35, 445–447.
4. Chahin, N., and Engel, A.G. (2008). Correlation of muscle biopsy, clinical course, and outcome in PM and sporadic IBM. *Neurology* 70, 418–424.
5. Griggs, R.C., Askanas, V., DiMauro, S., Engel, A., Karpati, G., Mendell, J.R., and Rowland, L.P. (1995). Inclusion body myositis and myopathies. *Ann. Neurol.* 38, 705–713.
6. Hilton-Jones, D., Miller, A., Parton, M., Holton, J., Sewry, C., and Hanna, M.G. (2010). Inclusion body myositis: MRC Centre for Neuromuscular Diseases, IBM workshop, London, 13 June 2008. *Neuromuscul. Disord.* 20, 142–147.
7. Greenberg, S.A., Pinkus, G.S., Amato, A.A., and Pinkus, J.L. (2007). Myeloid dendritic cells in inclusion-body myositis and polymyositis. *Muscle Nerve* 35, 17–23.
8. Karpati, G., Pouliot, Y., and Carpenter, S. (1988). Expression of immunoreactive major histocompatibility complex products in human skeletal muscles. *Ann. Neurol.* 23, 64–72.
9. Emslie-Smith, A.M., Arahata, K., and Engel, A.G. (1989). Major histocompatibility complex class I antigen expression, immunolocalization of interferon subtypes, and T cell-mediated cytotoxicity in myopathies. *Hum. Pathol.* 20, 224–231.
10. Mendell, J.R., Sahenk, Z., Gales, T., and Paul, L. (1991). Amyloid filaments in inclusion body myositis. Novel findings provide insight into nature of filaments. *Arch. Neurol.* 48, 1229–1234.

11. Santorelli, F.M., Sciacco, M., Tanji, K., Shanske, S., Vu, T.H., Golzi, V., Griggs, R.C., Mendell, J.R., Hays, A.P., Bertorini, T.E., et al. (1996). Multiple mitochondrial DNA deletions in sporadic inclusion body myositis: a study of 56 patients. *Ann. Neurol.* 39, 789–795.
12. Oldfors, A., Larsson, N.G., Lindberg, C., and Holme, E. (1993). Mitochondrial DNA deletions in inclusion body myositis. *Brain* 116, 325–336.
13. Simonetti, S., Chen, X., DiMauro, S., and Schon, E.A. (1992). Accumulation of deletions in human mitochondrial DNA during normal aging: analysis by quantitative PCR. *Biochim. Biophys. Acta* 1180, 113–122.
14. Banwell, B.L., and Engel, A.G. (2000). AlphaB-crystallin immunolocalization yields new insights into inclusion body myositis. *Neurology* 54, 1033–1041.
15. Muth, I.E., Barthel, K., Bähr, M., Dalakas, M.C., and Schmidt, J. (2009). Proinflammatory cell stress in sporadic inclusion body myositis muscle: over-expression of alphaB-crystallin is associated with amyloid precursor protein and accumulation of beta-amyloid. *J. Neurol. Neurosurg. Psychiatry* 80, 1344–1349.
16. Cox, F.M., Titulaer, M.J., Sont, J.K., Wintzen, A.R., Verschuuren, J.J., and Badrising, U.A. (2011). A 12-year follow-up in sporadic inclusion body myositis: an end stage with major disabilities. *Brain* 134, 3167–3175.
17. Benveniste, O., Guiguet, M., Freebody, J., Dubourg, O., Squier, W., Maissonobe, T., Stojkovic, T., Leite, M.I., Allenbach, Y., Herson, S., et al. (2011). Long-term observational study of sporadic inclusion body myositis. *Brain* 134, 3176–3184.
18. Lotz, B.P., Engel, A.G., Nishino, H., Stevens, J.C., and Litchy, W.J. (1989). Inclusion body myositis. Observations in 40 patients. *Brain* 112, 727–747.
19. Amato, A.A., Gronseth, G.S., Jackson, C.E., Wolfe, G.I., Katz, J.S., Bryan, W.W., and Barohn, R.J. (1996). Inclusion body myositis: clinical and pathological boundaries. *Ann. Neurol.* 40, 581–586.
20. Dalakas, M.C. (2004). Inflammatory disorders of muscle: progress in polymyositis, dermatomyositis and inclusion body myositis. *Curr. Opin. Neurol.* 17, 561–567.
21. Dimachkie, M.M., and Barohn, R.J. (2012). Inclusion body myositis. *Semin. Neurol.* 32, 237–245.
22. Dalakas, M.C., Sonies, B., Dambrosia, J., Sekul, E., Cupler, E., and Sivakumar, K. (1997). Treatment of inclusion-body myositis with IVIg: a double-blind, placebo-controlled study. *Neurology* 48, 712–716.
23. Dalakas, M.C., Koffman, B., Fujii, M., Spector, S., Sivakumar, K., and Cupler, E. (2001). A controlled study of intravenous immunoglobulin combined with prednisone in the treatment of IBM. *Neurology* 56, 323–327.
24. Muscle Study Group (2001). Randomized pilot trial of betaNF1a (Avonex) in patients with inclusion body myositis. *Neurology* 57, 1566–1570.
25. Muscle Study Group (2004). Randomized pilot trial of high-dose betaINF-1a in patients with inclusion body myositis. *Neurology* 63, 718–720.
26. Badrising, U.A., Maat-Schieman, M.L., Ferrari, M.D., Zwiderman, A.H., Wessels, J.A., Breedveld, F.C., van Doorn, P.A., van Engelen, B.G., Hoogendijk, J.E., Höweler, C.J., et al. (2002). Comparison of weakness progression in inclusion body myositis during treatment with methotrexate or placebo. *Ann. Neurol.* 51, 369–372.
27. Lindberg, C., Trysberg, E., Tarkowski, A., and Oldfors, A. (2003). Anti-T-lymphocyte globulin treatment in inclusion body myositis: a randomized pilot study. *Neurology* 61, 260–262.
28. Barohn, R.J., Herbelin, L., Kissel, J.T., King, W., McVey, A.L., Saperstein, D.S., and Mendell, J.R. (2006). Pilot trial of etanercept in the treatment of inclusion-body myositis. *Neurology* 66 (2, Suppl 1), S123–S124.
29. Dalakas, M.C., Rakocevic, G., Schmidt, J., Salajegheh, M., McElroy, B., Harris-Love, M.O., Shrader, J.A., Levy, E.W., Dambrosia, J., Kampen, R.L., et al. (2009). Effect of Alemtuzumab (CAMPATH 1-H) in patients with inclusion-body myositis. *Brain* 132, 1536–1544.
30. Sancricca, C., Mora, M., Ricci, E., Tonali, P.A., Mantegazza, R., and Mirabella, M. (2011). Pilot trial of simvastatin in the treatment of sporadic inclusion-body myositis. *Neurol. Sci.* 32, 841–847.
31. Amato, A.A., Sivakumar, K., Goyal, N., David, W.S., Salajegheh, M., Praestgaard, J., Lach-Trifilieff, E., Trendelenburg, A.U., Laurent, D., Glass, D.J., et al. (2014). Treatment of sporadic inclusion body myositis with bimagrumab. *Neurology* 83, 2239–2246.
32. McPherron, A.C., Lawler, A.M., and Lee, S.J. (1997). Regulation of skeletal muscle mass in mice by a new TGF-beta superfamily member. *Nature* 387, 83–90.
33. Lee, S.J. (2007). Quadrupling muscle mass in mice by targeting TGF-beta signaling pathways. *PLoS ONE* 2, e789.
34. Lin, S.Y., Morrison, J.R., Phillips, D.J., and de Kretser, D.M. (2003). Regulation of ovarian function by the TGF-beta superfamily and follistatin. *Reproduction* 126, 133–148.
35. Sugino, K., Kurosawa, N., Nakamura, T., Takio, K., Shimasaki, S., Ling, N., Titani, K., and Sugino, H. (1993). Molecular heterogeneity of follistatin, an activin-binding protein. Higher affinity of the carboxyl-terminal truncated forms for heparan sulfate proteoglycans on the ovarian granulosa cell. *J. Biol. Chem.* 268, 15579–15587.
36. Mendell, J.R., Sahenk, Z., Malik, V., Gomez, A.M., Flanigan, K.M., Lowes, L.P., Alfano, L.N., Berry, K., Meadows, E., Lewis, S., et al. (2015). A phase 1/2a follistatin gene therapy trial for becker muscular dystrophy. *Mol. Ther.* 23, 192–201.
37. Tawil, R., McDermott, M.P., Mendell, J.R., Kissel, J., and Griggs, R.C.; FSH-DY Group (1994). Facioscapulohumeral muscular dystrophy (FSHD): design of natural history study and results of baseline testing. *Neurology* 44, 442–446.
38. Mendell, J.R., Rodino-Klapac, L.R., Rosales-Quintero, X., Kota, J., Coley, B.D., Galloway, G., Craenen, J.M., Lewis, S., Malik, V., Shilling, C., et al. (2009). Limb-girdle muscular dystrophy type 2D gene therapy restores alpha-sarcoglycan and associated proteins. *Ann. Neurol.* 66, 290–297.
39. Mendell, J.R., Rodino-Klapac, L.R., Rosales, X.Q., Coley, B.D., Galloway, G., Lewis, S., Malik, V., Shilling, C., Byrne, B.J., Conlon, T., et al. (2010). Sustained alpha-sarcoglycan gene expression after gene transfer in limb-girdle muscular dystrophy, type 2D. *Ann. Neurol.* 68, 629–638.
40. Viollet, L., Gailey, S., Thornton, D.J., Friedman, N.R., Flanigan, K.M., Mahan, J.D., and Mendell, J.R. (2009). Utility of cystatin C to monitor renal function in Duchenne muscular dystrophy. *Muscle Nerve* 40, 438–442.
41. Hawley, R.J., Jr., Schellinger, D., and O'Doherty, D.S. (1984). Computed tomographic patterns of muscles in neuromuscular diseases. *Arch. Neurol.* 41, 383–387.
42. Mercuri, E., Talim, B., Moghadaszadeh, B., Petit, N., Brockington, M., Counsell, S., Guicheney, P., Muntoni, F., and Merlini, L. (2002). Clinical and imaging findings in six cases of congenital muscular dystrophy with rigid spine syndrome linked to chromosome 1p (RSM1). *Neuromuscul. Disord.* 12, 631–638.
43. Kinali, M., Arechavala-Gomez, V., Cirak, S., Glover, A., Guglieri, M., Feng, L., Hollingsworth, K.G., Hunt, D., Jungbluth, H., Roper, H.P., et al. (2011). Muscle histology vs MRI in Duchenne muscular dystrophy. *Neurology* 76, 346–353.
44. Hansen, J., Brandt, C., Nielsen, A.R., Hojman, P., Whitham, M., Febbraio, M.A., Pedersen, B.K., and Plomgaard, P. (2011). Exercise induces a marked increase in plasma follistatin: evidence that follistatin is a contraction-induced hepatokine. *Endocrinology* 152, 164–171.
45. Morita, M., Gravel, S.P., Hulea, L., Larsson, O., Pollak, M., St-Pierre, J., and Topisirovic, I. (2015). mTOR coordinates protein synthesis, mitochondrial activity and proliferation. *Cell Cycle* 14, 473–480.
46. Winbanks, C.E., Weeks, K.L., Thomson, R.E., Sepulveda, P.V., Beyer, C., Qian, H., Chen, J.L., Allen, J.M., Lancaster, G.I., Febbraio, M.A., et al. (2012). Follistatin-mediated skeletal muscle hypertrophy is regulated by Smad3 and mTOR independently of myostatin. *J. Cell Biol.* 197, 997–1008.
47. Mihaylova, M.M., and Shaw, R.J. (2011). The AMPK signalling pathway coordinates cell growth, autophagy and metabolism. *Nat. Cell Biol.* 13, 1016–1023.
48. Mounier, R., Thérêt, M., Lantier, L., Foretz, M., and Viollet, B. (2015). Expanding roles for AMPK in skeletal muscle plasticity. *Trends Endocrinol. Metab.* 26, 275–286.
49. Phillips, D.J., de Kretser, D.M., and Hedger, M.P. (2009). Activin and related proteins in inflammation: not just interested bystanders. *Cytokine Growth Factor Rev.* 20, 153–164.
50. Li, Z.B., Kollias, H.D., and Wagner, K.R. (2008). Myostatin directly regulates skeletal muscle fibrosis. *J. Biol. Chem.* 283, 19371–19378.
51. Zhu, J., Li, Y., Lu, A., Gharaibeh, B., Ma, J., Kobayashi, T., Quintero, A.J., and Huard, J. (2011). Follistatin improves skeletal muscle healing after injury and disease through

- an interaction with muscle regeneration, angiogenesis, and fibrosis. *Am. J. Pathol.* 179, 915–930.
52. Dong, Y., Pan, J.S., and Zhang, L. (2013). Myostatin suppression of Akirin1 mediates glucocorticoid-induced satellite cell dysfunction. *PLoS ONE* 8, e58554.
53. Jorgensen, A.N., Aagaard, P., Nielsen, J.L., Frandsen, U., and Diederichsen, L.P. (2016). Effects of blood-flow-restricted resistance training on muscle function in a 74-year-old male with sporadic inclusion body myositis: a case report. *Clin. Phys. Funct. Imaging* 36, 504–509.
54. Johnson, L.G., Collier, K.E., Edwards, D.J., Philippe, D.L., Eastwood, P.R., Walters, S.E., Thickbroom, G.W., and Mastaglia, F.L. (2009). Improvement in aerobic capacity after an exercise program in sporadic inclusion body myositis. *J. Clin. Neuromuscul. Dis.* 10, 178–184.